

## Supporting Information

# Dielectrophoretic medium exchange around droplets for on-chip fabrication of Layer-by-Layer microcapsules

Haizhen Sun<sup>1</sup>, Yukun Ren<sup>1,2,\*</sup>, Tianyi Jiang<sup>1</sup>, Ye Tao<sup>1</sup>, Hongyuan Jiang<sup>1,\*</sup>

<sup>1</sup> School of Mechatronics Engineering, Harbin Institute of Technology, West Da-zhi Street 92, Harbin, Heilongjiang, PR China 150001.

<sup>2</sup> State Key Laboratory of Robotics and System, Harbin Institute of Technology, West Da-zhi Street 92, Harbin, Heilongjiang, PR China 150001.

\*E-mail: [rykhit@hit.edu.cn](mailto:rykhit@hit.edu.cn)

\*E-mail: [jhy\\_hit@hit.edu.cn](mailto:jhy_hit@hit.edu.cn)

Electronic Supporting Information (ESI)

**This material gives supporting information for the model studied in the paper.**

Section S1. The simulation model and boundary conditions

Section S2. The electric field profile around the electrode

Section S3. The critical flow rate and voltage for two-particle isolation

Section S3. Multimode medium exchange for three different particles

### **Additional Supplementary Material (AVI):**

Movie S1: Droplet purification (AVI)

Movie S2: Multimodal medium exchange around two different particles (AVI)

Movie S3: Isolation of three particles with different sizes (AVI)

Movie S4: On-chip generation of Layer-by-Layer microcapsules (AVI)

## Section S1. The simulation model and boundary conditions

A 3-D model of the same size as the experimental chip was established, and the boundary conditions for the simulation space are shown in Figure S1.<sup>1-4</sup>

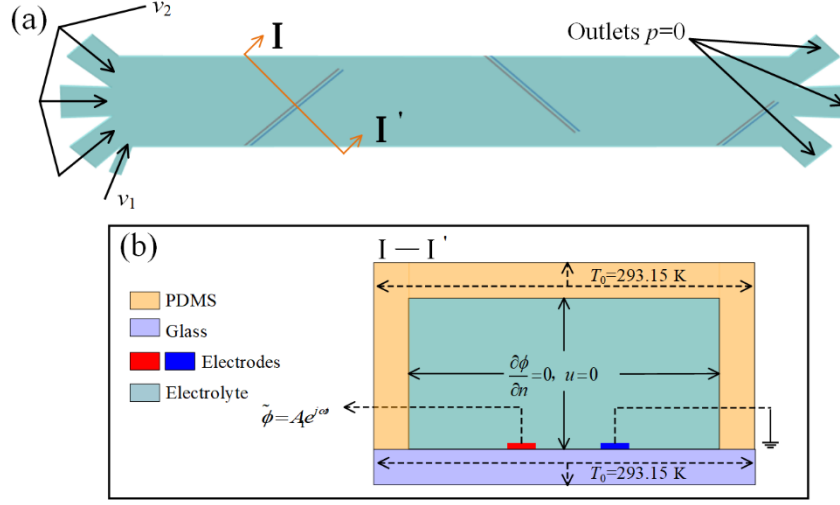


Figure S1 Schematic diagram of the (a) 3-D simulation model and (b) the corresponding boundary conditions.

The details of governing equations and boundary conditions used in the numerical simulation are given below:

At the electrode surface of negligible thickness (transparent to heat transfer), we have:

$$\phi = A_1 e^{j\omega t}; \quad v_x = v_y = v_z = 0 \quad (\text{S1})$$

At the inlet of the channel:

$$\frac{\partial \phi}{\partial n} = 0; \quad T_{\text{fluid}} = T_0; \quad v_{x1} = v_1(y, z); \quad v_{x2} = v_2(y, z) \quad (\text{S2})$$

At the outlet of the channel:

$$\frac{\partial \phi}{\partial n} = 0; \quad \frac{\partial T_{\text{fluid}}}{\partial n} = 0; \quad p = 0 \quad (\text{S3})$$

At the interface between the PDMS cover and electrolyte media:

$$\frac{\partial \phi}{\partial n} = 0; \quad T_{\text{fluid}} = T_{\text{PDMS}}; \quad k_{\text{fluid}} \frac{\partial T_{\text{fluid}}}{\partial n} = k_{\text{PDMS}} \frac{\partial T_{\text{PDMS}}}{\partial n}; \quad v_x = v_y = v_z = 0 \quad (\text{S4})$$

At the interface between the glass substrate and electrolyte media:

$$\frac{\partial \phi}{\partial n} = 0; \quad T_{\text{fluid}} = T_{\text{glass}}; \quad k_{\text{fluid}} \frac{\partial T_{\text{fluid}}}{\partial n} = k_{\text{glass}} \frac{\partial T_{\text{glass}}}{\partial n}; \quad v_x = v_y = v_z = 0 \quad (\text{S5})$$

At the top surface of PDMS cover:

$$T_{\text{PDMS}} = T_0 \quad (\text{S6})$$

At the bottom surface of glass substrate:

$$T_{\text{glass}} = T_0 \quad (\text{S7})$$

here  $n$  is the local unit normal vector on the interface,  $p$  is the fluid pressure at the outlet,  $k_{\text{fluid}}=0.6(\text{W} / \text{mK})$  is thermal conductivity of fluid sample,  $k_{\text{PDMS}}=0.2(\text{W} / \text{mK})$  is the thermal conductivity of PDMS cover,  $k_{\text{glass}}=1.1(\text{W} / \text{mK})$  is the thermal conductivity of glass substrate. Where  $T_{\text{fluid}}$ ,  $T_{\text{PDMS}}$  and  $T_{\text{glass}}$  represent the temperate field inside the liquid media, PDMS cover and glass substrate, respectively.

### Section S2. The electric field profile around the electrodes

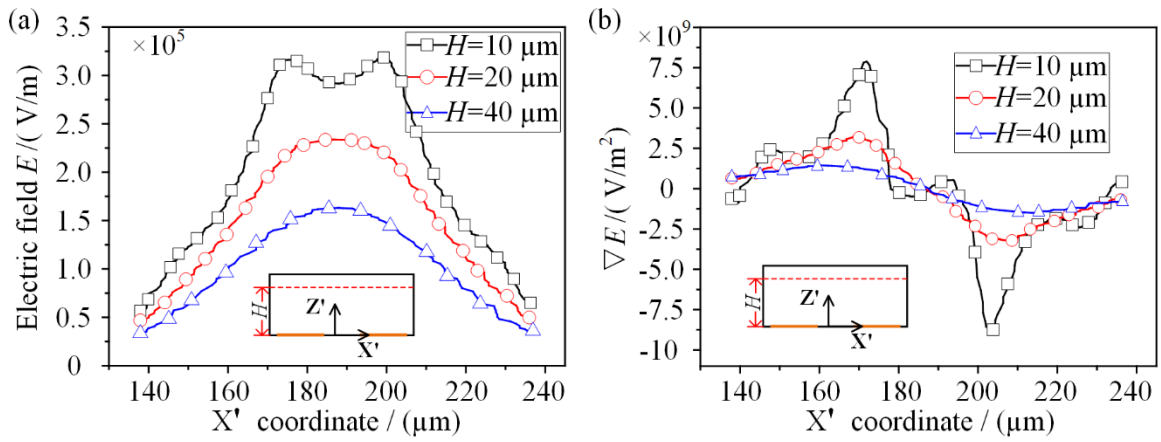


Figure S2 Changes in (a) the simulated electric field and (b) the corresponding gradient along a line above the electrodes.

The electric field and its gradient were numerically calculated, as shown in Figure S2. It is clear that the highest electric field arises in the vicinity of adjacent electrode edges, as shown in Figure S2a. The intensity of the electric field decreases significantly at the regions away from the electrode edges. The gradient of the electric field, which determines the magnitude of dielectrophoretic force, behaves the same trend as the electric field, as shown in Figure S2b. It shows two peaks of gradient along the line at the cross section, predicting that the DEP force gains the maximum in the same position.

### Section S3. The critical flow rate and voltage for two-particle isolation

An appropriate combination of inlet flow rate and applied voltage contributing to isolating different particles into independent medium, as shown in Figure S3. It is clearly that the critical voltage shows a linear increase with the inlet flow rate.

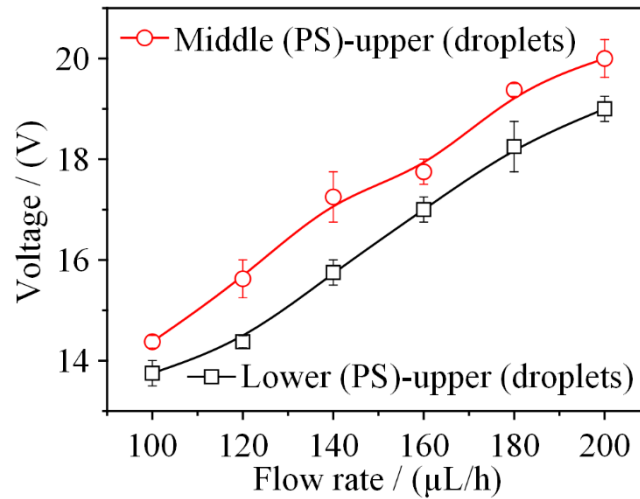


Figure S3 The red line with circle labelling represents critical value for that PS particles are transported into the middle medium while droplets are railed into the upper medium. The black line with square labeling is the critical value for that PS particles exit from the lower medium and droplets enter the upper medium.

### Section S3. Multimode medium exchange for three different particles

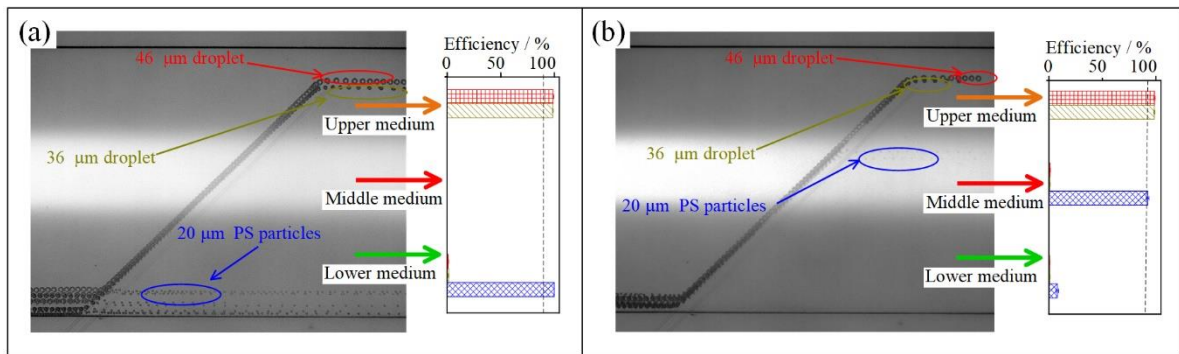


Figure S4 Multimode medium exchange for three different particles. (a) Both droplets were transferred to the upper medium while the PS particles were escaped at the lower medium at  $A_1 = 12.5$  V. (b) Both droplets were transported to the upper medium while PS particles migrated into the middle medium at 16.25 V

### REFERENCES

- (1) Ramos, A.; Morgan, H.; Green, N. G.; Castellanos, A. The role of electrohydrodynamic forces in the dielectrophoretic manipulation and separation of particles. *Journal of Electrostatics* **1999**, *47* (1-2), 71-81.
- (2) Xuan, X. Joule heating in electrokinetic flow. *Electrophoresis* **2008**, *29* (1), 33-43.
- (3) Garcia-Sanchez, P.; Ramos, A.; Mugele, F. Electrothermally driven flows in ac electrowetting. *Physical review. E, Statistical, nonlinear, and soft matter physics* **2010**, *81* (1 Pt 2), 015303.
- (4) Liu, W.; Ren, Y.; Tao, Y.; Yao, B.; Li, Y. Simulation analysis of rectifying microfluidic mixing with field-effect-tunable electrothermal induced flow. *Electrophoresis* **2018**, *39* (5-6), 779-793.